Smith, C. C. (2005). *Géotechnique* **55**, No. 8, 607–612

TECHNICAL NOTE

Complete limiting stress solutions for the bearing capacity of strip footings on a Mohr–Coulomb soil

C. C. SMITH*

KEYWORDS: bearing capacity; footings; limit state design/analysis; plasticity

INTRODUCTION

The method of characteristics is used to develop equilibrium limiting stress solutions for the problem of the vertical bearing capacity of strip footings on cohesionless soils. This note extends and completes the solutions of Lundgren & Mortenson (1953) by demonstrating the existence of equilibrium stress fields nowhere violating yield

(*a*) for the rigid wedge of soil beneath the footing (where present)
(*b*) everywhere outside the main failure zone.

The solutions presented are thus demonstrated as rigorous lower bounds for an associative material. Resulting N_γ values are compared with those in the literature and show good agreement with recently published numerical limit analyses. Pressure distributions beneath the footings are also compared with the elastic Boussinesq analysis and the load spreading assumption, and show significant differences.

PROBLEM DEFINITION

It is required to find an equilibrium stress field nowhere violating yield beneath a rigid footing of width B carrying a uniform vertical stress p and resting on the horizontal surface of a uniform body of cohesionless soil of unit weight γ. The surface of the soil adjacent to the footing carries a surcharge load $q \geqslant 0$. The solution should maximise p and will depend on three dimensionless parameters: the angle of shearing resistance of the soil ϕ, the roughness of the base δ, and the ratio $q/\gamma B$.

Classically the parameters are related as follows:

$$p = \mu\left(qN_q + \frac{1}{2}\gamma BN_\gamma\right) \tag{1}$$

where $N_q = N_q(\phi)$, $N_\gamma = N_\gamma(\phi, \delta)$ and $\mu = \mu(\phi, \delta, q/\gamma B)$. Conventionally μ is taken as 1. It is identically 1 for $q/\gamma B = 0$ or ∞, and the assumption of $\mu = 1$ for $0 < q/\gamma B < \infty$ has been shown to be conservative by several authors (e.g. Bolton & Lau, 1993). Bolton & Lau (1993) also demonstrate how any solution based on a constant-ϕ relationship can be straightforwardly extended to the more general (c, ϕ) envelope.

Following the notation of Sokolovski (1965), the key equations of equilibrium and yield relating normal (σ) and shear (τ) stresses in the soil are:

$$\frac{\partial\sigma_x}{\partial x} + \frac{\partial\tau_{xy}}{\partial y} = 0 \tag{2}$$

$$\frac{\partial\tau_{xy}}{\partial x} + \frac{\partial\sigma_y}{\partial y} = \gamma \tag{3}$$

and

$$\frac{1}{4}(\sigma_x - \sigma_y)^2 + \tau_{xy}^2 = \frac{\sin^2\phi}{4}(\sigma_x + \sigma_y)^2 \tag{4}$$

where the adopted coordinate system in relation to the footing is depicted in Fig. 1.

Equation 4 may alternatively be expressed as follows

$$\left.\begin{matrix}\sigma_x\\ \sigma_y\end{matrix}\right\} = \sigma(1 \pm \sin\phi\cos 2\varphi) \tag{5}$$

$$\tau_{xy} = \sigma\sin\phi\sin 2\varphi \tag{6}$$

where σ is the mean stress and φ is the angle between the major principal stress direction and the horizontal (anticlockwise positive), as illustrated in Fig. 1.

Equations (5) and (6) are substituted into equations (2) and (3) to yield the following ordinary differential equations along the characteristics of the limiting stress field:

$$\mathrm{d}y = \mathrm{d}x\tan(\varphi\mu\varepsilon) \tag{7}$$

$$\mathrm{d}\sigma\mu 2\sigma\tan\phi\,\mathrm{d}\varphi = \gamma(\mathrm{d}y\tan\phi\mu\mathrm{d}x) \tag{8}$$

where

$$\varepsilon = \frac{\pi}{4} - \frac{\phi}{2} \tag{9}$$

The nature of the stress field underlying the footing is strongly influenced by the symmetry condition that requires that the major principal stress direction be vertical on the centreline through the footing ($\varphi = 90°$).

NATURE OF STRESS STATE IMMEDIATELY BELOW FOOTING

Weightless soil with a surface load

When $\gamma = 0$ and the base is smooth, the well-documented solution depicted in Fig. 2(a) is straightforward, and requires no further discussion. Such a twin deformation zone mechanism for a smooth footing has been observed in experiments by Ko & Davison (1973).

For a fully rough base, $\delta = \phi$, it is tempting to consider that the fan zone can be continued round to the footing base, mobilising full friction there (thereby achieving a higher load capacity). However, the symmetry condition dictates that the fan zone solution can be continued only as far as the characteristic emanating from the footing edge that meets the footing centreline with major principal stress direction vertical ($\varphi = 90°$). Beyond this the stress field must account for the symmetry condition. The only possible simple *limiting* stress field for the remaining soil wedge will therefore be a Rankine state with $\varphi = 90°$. This, however, requires that zero shear be mobilised on the footing soil

Manuscript received 17 November 2004; revised manuscript accepted 5 July 2005.
Discussion on this paper closes on 1 April 2006, for further details see p. ii.
* Geotechnics Research Group, Department of Civil and Structural Engineering, University of Sheffield, UK.

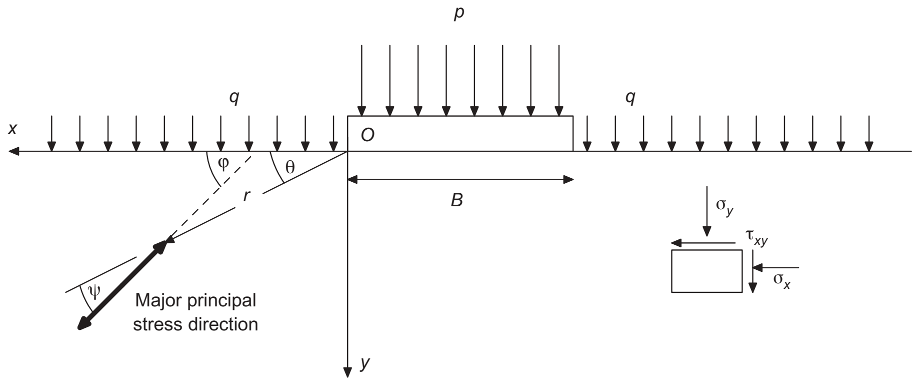

Fig. 1. Coordinate system for footing analysis

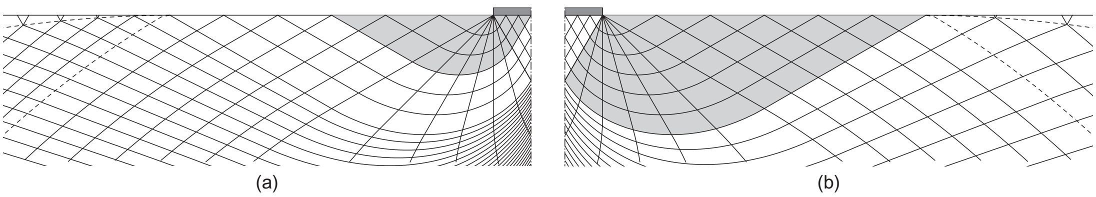

Fig. 2. Characteristic lines under smooth and rough bases for $q/\gamma B = \infty$, $\phi = 30°$: (a) smooth; (b) rough Shaded area indicates yielding zone. Discontinuities are denoted by dashed lines

interface. The wedge stress state cannot therefore be limiting, and the wedge itself will be rigid. It remains to demonstrate that a non-limiting stress state is possible within the wedge. A trivial solution is given by the Rankine stress state itself and is depicted in Fig. 2(b). Such single-wedge mechanisms for rough footings have also been observed experimentally by Ko & Davison (1973).

Such solutions are relevant to scenarios where the surface loads p are very large relative to γB.

Soil possessing weight with no surface load

In this case all rupture lines are similar with O as the point of similarity. The solution for the stress field uninfluenced by the footing symmetry conditions follows from the solution of the simultaneous ordinary differential equations of equilibrium and yield in polar coordinates. Following the notation of Sokolovski (1965) these may be expressed as follows:

$$\frac{\partial \chi}{\mathrm{d}\theta} = \frac{\cos(2\psi + \theta) + \chi \sin 2\psi}{\cos 2\psi - \sin\phi} \tag{10}$$

and

$$\frac{\partial \psi}{\mathrm{d}\theta} + 1 = \frac{\sin\theta - \sin\phi \sin(2\psi + \theta) - \chi \cos^2\phi}{2\chi \sin\phi(\cos 2\psi - \sin\phi)} \tag{11}$$

where

$$\sigma = \gamma r \chi \tag{12}$$

$$\psi = \varphi - \theta \tag{13}$$

and $\psi = \psi(\theta)$, $\chi = \chi(\theta)$, and θ is measured anticlockwise from the x-axis, as depicted in Fig. 1.

Equations (10) and (11) are solved from $\theta_1 = \varepsilon$ to θ_2, where θ_2 defines the edge of the yielding zone, which may be either at the base of the footing or at the edge of a rigid wedge where this is assumed. The boundary conditions at θ_1 are $\psi = -\varepsilon$, $\chi = 1/2\sin\varepsilon$. Solution of equations (10) and (11) at this boundary is complex, owing to a singularity, and is discussed in detail by Heurtaux (1959).

For a smooth footing the solution (as described by Lundgren & Mortenson, 1953, and other authors) is straightforward, and is depicted in Fig. 3(a). The solution is solved such that $\psi = -\pi/2$ on the base of the footing ($\theta_2 = \pi$), and there is no rigid wedge beneath the footing. For a fully rough footing, the nature of the wedge underlying the footing has been the subject of various assumptions by a number of researchers. Two scenarios will be examined. Several authors (e.g. Bolton & Lau, 1993; Zhu *et al.*, 2003)

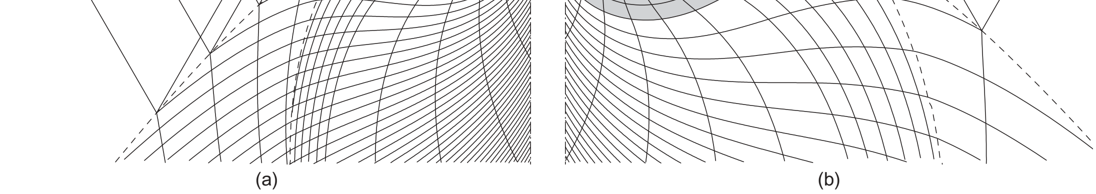

Fig. 3. Characteristic lines under smooth and rough bases for $q/\gamma B = 0$, $\phi = 30°$: (a) smooth; (b) rough Shaded area indicates yielding zone. Discontinuities are denoted by dashed lines

assumed a wedge base angle of ($\pi/4 + \phi/2$) consistent with the weightless soil case, and solved the characteristic equations such that full shear strength was mobilised at this angle: that is, the characteristic was tangential to this surface with $\psi = -\varepsilon$ at $\theta_2 = 3\pi - \phi/2$. In contrast, Lundgren & Mortenson (1953) computed the characteristics all the way to the base of the footing ($\theta_2 = \pi$), again assuming full shear strength mobilised at this interface ($\psi = -\varepsilon$). They then assumed a rigid wedge delineated by the characteristic that emanates from the edge of the footing and meets the symmetry line with its major principal stress direction vertical as required. In both cases it was assumed, but not confirmed, that an equilibrium non-yielding stress state was possible within the wedge.

To investigate this further it is of value to examine equation (11) in the vicinity of θ_2, by recasting ψ in terms of a new variable f such that

$$\psi = -\varepsilon + f \tag{14}$$

giving

$$\frac{\partial f}{\mathrm{d}\theta} = -1 + \frac{\sin\theta - \sin\phi\sin(2\varepsilon + 2f + \theta) - \chi\cos^2\phi}{4f\chi\sin\phi\cos\phi} \tag{15}$$

At $\theta = \theta_2$, χ is large, and so the equation may be approximated by

$$\frac{\mathrm{d}f}{\mathrm{d}\theta} \approx -1 - \frac{\cot\phi}{4f} \tag{16}$$

As $\theta \to \theta_2$ ($\theta \leqslant \theta_2$), $f \to 0$ ($f \leqslant 0$). A negative value of f corresponds to a positive value of $\mathrm{d}f/\mathrm{d}\theta$ as required. However, contradictory conditions are obtained as θ increases past θ_2: if f continues to increase, f is positive and $\mathrm{d}f/\mathrm{d}\theta < 0$; likewise if f decreases, f is negative and $\mathrm{d}f/\mathrm{d}\theta > 0$. The solution has thus reached a limit, and it is not possible to progress it further. Unlike the boundary at θ_1 the extreme stress state reached at θ_2 is the limit of that which can be sustained by the soil mobilising its full strength.

As equations (10) and (11) apply always in the vicinity of the footing edge, simple equilibrium non-yielding stress states are therefore not possible at the footing edge and thus within the wedge for any value of $\theta_2 < \pi$. This indicates that the results of Bolton & Lau (1993) and Zhu *et al.* (2003) are incorrect, and would be admissible only if the rigid footing itself extended into the area of the wedge and could mobilise full friction at the soil/footing interface.

The implication of this is that the maximum load from this type of solution can be achieved only assuming full friction mobilised at $\theta_2 = \pi$ on the edge of the footing base, with rigid wedge as defined by Lundgren & Mortenson (1953) and as illustrated in Fig. 3(b). However, it is still necessary to demonstrate the existence of a non-yielding equilibrium stress state for this wedge.

It is in fact possible to derive a full limiting solution for this zone, as illustrated in Fig. 4. The α characteristic ABC is solved to D using the symmetry condition. The β characteristic may then be solved to the surface at E. The process is then repeated until the whole wedge is solved. The mobilised shearing angle on the footing base increases from zero at the footing centre to ϕ at the edge. Thus although limiting conditions could be assumed present in the soil, they do not exist on the footing base, and this thus requires the wedge of soil to act as a rigid body.

Such solutions may be extended to the case where the footing roughness $\delta < \phi$. The solution is solved such that $\psi = -\pi/2 - (\Delta + \delta)/2$ on the base of the footing, where $\sin\Delta = \sin\delta/\sin\phi$. Fig. 5 shows an example of this for a foundation with roughness $\delta = \phi/2$. The symmetry condition requirement results in a smaller wedge. As $\delta \to 0$, the wedge shrinks nearer to the footing centre until it vanishes at $\delta = 0$.

EXISTENCE OF AN EQUILIBRIUM NON-YIELDING STRESS FIELD OUTSIDE MAIN FAILURE ZONE

The stress fields described above are theoretically valid only if it can be established that an equilibrium stress field nowhere violating yield exists outside the main failure zone. In general this stress field will be non-limiting, though where collapse is occurring beneath the surface load, such as in the case of sand overlying soft clay or of backfill overlying a collapsing void, such stress fields will be at least partially limiting in extent.

It is possible to derive a fully limiting equilibrium stress field (excepting stress discontinuities) outside the main failure zone, thus satisfying the above requirements as illustrated in Fig. 4. The line of symmetry gives a condition by which a β-characteristic may be continued outside the main failure zone from points O, P to Q on the symmetry line. An α-characteristic may then be solved to point R. It passes through a weak discontinuity at this point and then may be continued to point S, where the line XS is a discontinuity with the stress state to the left of XS a simple Rankine state with major principal stress direction vertical. Repetition of this process thus generates a full equilibrium stress field as depicted in Figs 2 and 3. Fig. 6 shows the development of the stress characteristics (for $\phi = 30°$) into the far field for a smooth footing for the two cases $q/\gamma B = \infty$ and $q/\gamma B = 0$. These are plotted to the depth where the first discontinuity (XR in Fig. 4) meets the line of symmetry. At this point, the discontinuity will cross its mirror image on the symmetry line and continue further downwards. The second discontinuity (XS in Fig. 4) asymptotically approaches the angle π-ε

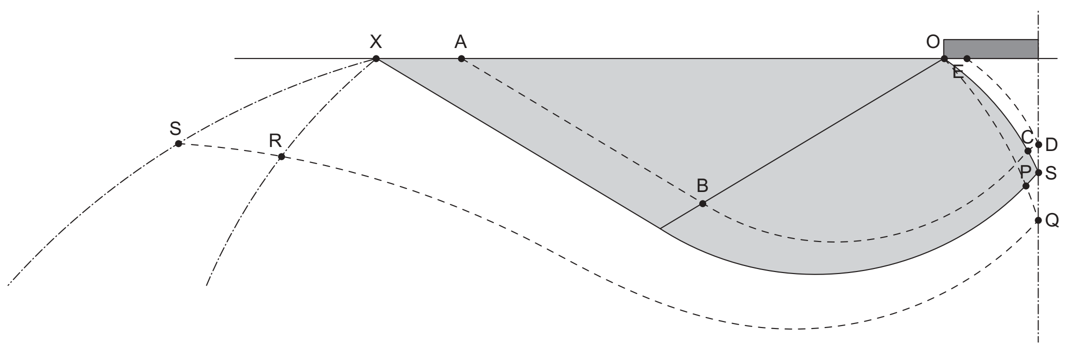

Fig. 4. Construction of characteristic network for equilibrium stress field outside main failure zone. Shaded area indicates yielding zone

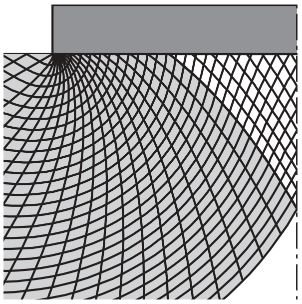

Fig. 5. Characteristics immediately beneath footing for footing roughness $\delta = \phi/2$, $q/\gamma B = 0$, and $\phi = 30°$. Shaded area indicates yielding zone.

to the horizontal (i.e. the simple Rankine state with major principal stress vertical that lies beyond the discontinuity). Similar behaviour is seen for rough footings. The stress fields are thus extensible everywhere and tend to a simple Rankine state with major principal stress vertical in the extended far field both laterally and vertically.

BEARING CAPACITY FACTOR N_γ

Table 1 enumerates the N_γ footing pressures for the three cases $\delta/\phi = 0$, 0·5 and 1. Lundgren & Mortenson (1953) presented only one result for $\phi = 30°$ in their paper. However, Hansen & Christensen (1969) graphically presented additional results based on the same method. The results for fully smooth and fully rough footings are in excellent agreement with Hansen & Christensen (1969), and also with more recent results computed using the method of characteristics (rather than equations (10) and (11)) using the ABC program described by Martin (2003a, 2003b). As extension of an equilibrium stress field has now been demonstrated throughout the soil, the results are confirmed as true lower bounds (for an associative material). These results are often taken as the actual solution. It is beyond the scope of this note to demonstrate this with a full analysis involving corresponding upper bounds, but strong supporting evidence comes from the recent data of Hjiaj *et al.* (2005), who present upper- and lower-bound solutions from numerical limit analysis (given in Table 1) that very closely bracket the values presented. Table 1 also compares the current values of N_γ with current recommendations in Eurocode 7 (1995):

$$N_\gamma = 2{\cdot}0(N_q - 1)\tan\phi \tag{17}$$

where

$$N_q = \exp(\pi\tan\phi)\tan^2\left(45 + \frac{\phi}{2}\right) \tag{18}$$

This equation overestimates N_γ by up to 40%, or returns values of N_γ equivalent to angles of shearing resistance ϕ up to 2° higher.

An empirical search for a better fit using a similar form of equations indicates that those below are a more suitable formulation:

$$N_\gamma = 1{\cdot}75\left(N'_q - 1\right)\tan\phi \tag{19}$$

where

$$N'_q = \exp\left[(0{\cdot}75\pi + \phi)\tan\phi\right]\tan^2\left(45 + \frac{\phi}{2}\right) \tag{20}$$

Predictions using this equation are given in Table 1. These give results within 1% of the current theory over the range $\phi = 20$–$50°$. The error increases to a 3% underestimate at $\phi = 15°$ and $\phi = 55°$. Table 1 also examines the values of N_γ predicted by Bolton & Lau (1993). It is clear that, for the rough footing, the assumption of a predefined wedge of soil beneath the footing leads to a significant and unsafe overestimate of the bearing capacity and an incorrect lower bound.

SOLUTIONS FOR SOIL POSSESSING WEIGHT WITH SURFACE LOAD

Scenarios of this nature ($0 < q/\gamma B < \infty$) result in solutions part way between the two extreme cases already considered. Values of μ as defined by equation (1) are plotted against $\gamma B/q$ for various values of ϕ in Fig. 7 for a fully rough footing. It is seen that the error in using equation (1) with $\mu = 1$ is no more than 25% at worst. The values derived here are slightly larger than those derived by Lundgren & Mortenson (1953), but peak at the same value of $\gamma B/q$.

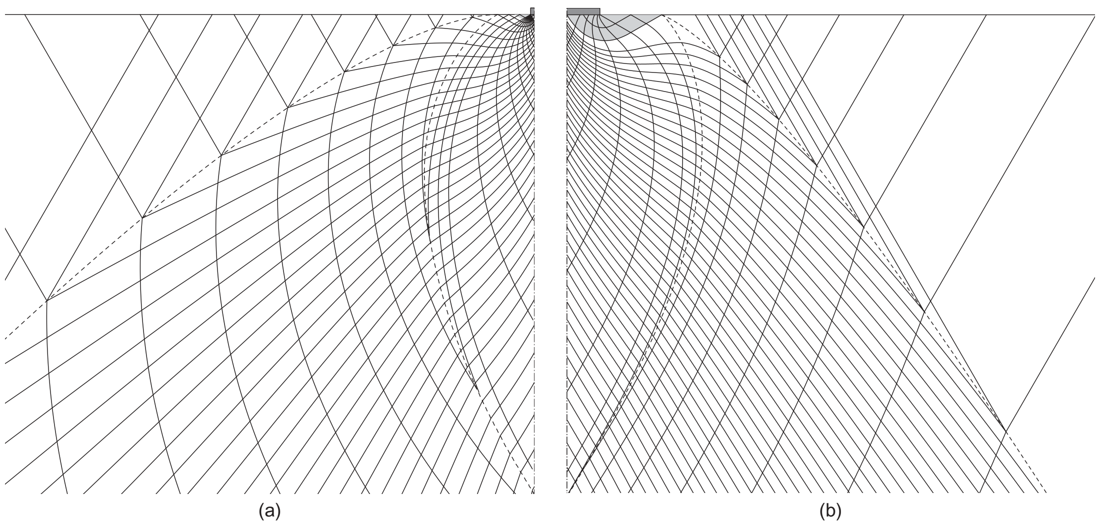

Fig. 6. Extended stress field under smooth bases for (a) $q/\gamma B = \infty$ (illustrated depth 63B) and (b) $q/\gamma B = 0$ (illustrated depth 7·3B); $\phi = 30°$. Shaded area indicates yielding zone. Discontinuities are denoted by dashed lines

Table 1. Bearing capacity factor N_γ

ϕ	Smooth $\delta = 0$			$\delta = \phi/2$	Rough $\delta = \phi$				
	Current theory	Hjiaj *et al.* (2005)	Bolton & Lau (1993)	Current theory	Current theory	Hjiaj *et al.* (2005)	Bolton & Lau (1993)	Eqn ;1;(18)	Eqn ;1;(20)
15	0·70	0·70–0·74	0·71	0·99	1·18	1·18–1·24	3·17	1·82	1·14
20	1·58	1·58–1·67	1·60	2·41	2·84	2·82–2·96	5·97	3·93	2·84
25	3·46	3·45–3·65	3·51	5·63	6·49	6·43–6·74	11·6	9·01	6·58
26	4·05			6·66	7·64			10·6	7·75
27	4·74			7·88	9·00			12·4	9·14
28	5·56			9·34	10·6			14·6	10·8
29	6·52			11·1	12·5			17·1	12·7
30	7·65	7·62–8·08	7·74	13·1	14·8	14·6–15·2	23·6	20·1	15·0
31	9·00		9·10	15·6	17·4		27·4	23·6	17·7
32	10·6		10·7	18·6	20·6		31·8	27·7	20·9
33	12·5		12·7	22·1	24·4		37·1	32·6	24·7
34	14·8		15·0	26·4	29·0		43·5	38·4	29·3
35	17·6	17·5–18·5	17·8	31·6	34·5	34·0–35·6	51·0	45·2	34·9
36	20·9		21·0	37·9	41·1		60·0	53·4	41·6
37	24·9		25·0	45·6	49·1		71·0	63·2	49·6
38	29·8		30·0	54·9	58·9		85·0	74·9	59·4
39	35·8		36·0	66·4	70·9		101	89·0	71·4
40	43·2	42·8–45·4	44·0	80·6	85·6	83·3–88·4	121	106	86·1
41	52·3		53·0	98·2	104		145	127	104
42	63·5		65·0	120	126		176	152	127
43	77·6		79·0	148	154		214	183	155
44	95·3		97·0	182	190		262	221	190
45	118	116–123	120	226	234	225–241	324	268	234
46	146		150	282	291		402	326	291
47	182		188	354	364		505	399	363
48	230		237	447	458		638	492	456
49	291		302	568	581		815	609	577
50	372		389	729	743		1052	758	736
51	480		505	942	958		1373	951	947
52	624		663	1230	1247		1812	1201	1230
53	820			1621	1640			1530	1612
54	1091			2159	2180			1966	2136
55	1467			2910	2933			2549	2863

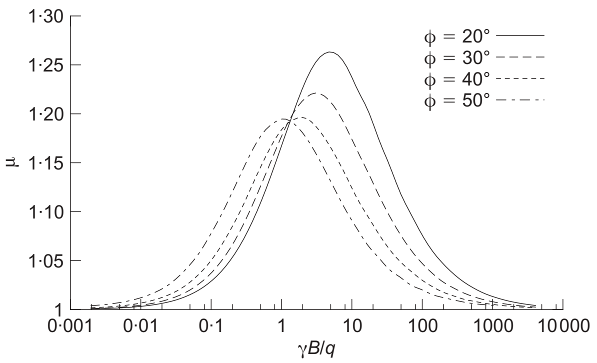

Fig. 7. Variation of μ with $\gamma B/q$ for fully rough footing for various values of ϕ

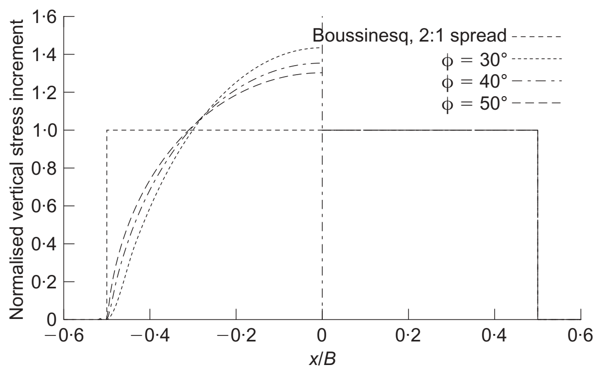

Fig. 8. Normalised vertical stress increment distributions acting immediately beneath rough footing. Left-hand side, $q/\gamma B = 0$; right-hand side, $q/\gamma B = \infty$

PRESSURE DISTRIBUTIONS BENEATH FOOTINGS

The solutions derived above permit examination of the pressure distributions under footings at their failure load. These distributions will be valid in the yielding zone, and would be expected to be approximated well by the derived stress fields in the zones assumed to be non-yielding, particularly close to the yielding zones. Horizontal profiles of vertical stress increment are presented for depths 0, B, $2B$ in Figs 8, 9 and 10, for values of $\phi = 30°$, 40° and 50°, together with the profiles from both a Boussinesq and a 2 vertical : 1 horizontal load spreading analysis for comparison. These are presented for the two extreme cases of weightless soil with surface surcharge and soil possessing weight with no surface surcharge. All loads are normalised by the average footing stress p. For the soil possessing weight with no surface surcharge, the vertical stress increases to a peak part way down the wedge before subsequently decreasing with depth. It can also be seen that the plastic solutions result in significantly more severe concentrated pressure distributions than given by the Boussinesq or load spread models. The strongest soils give the highest stress concentra-

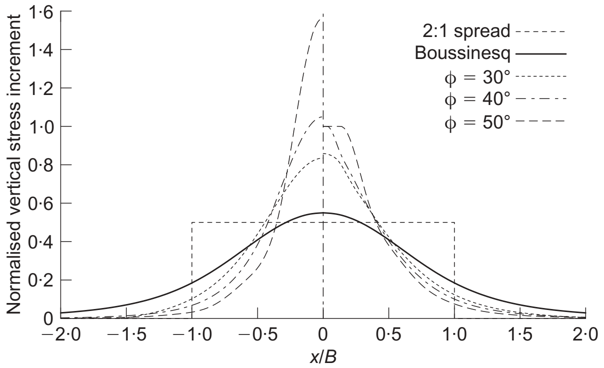

Fig. 9. Normalised vertical stress increment distributions acting at depth B beneath rough footing. Left-hand side, $q/\gamma B = 0$; right-hand side, $q/\gamma B = \infty$

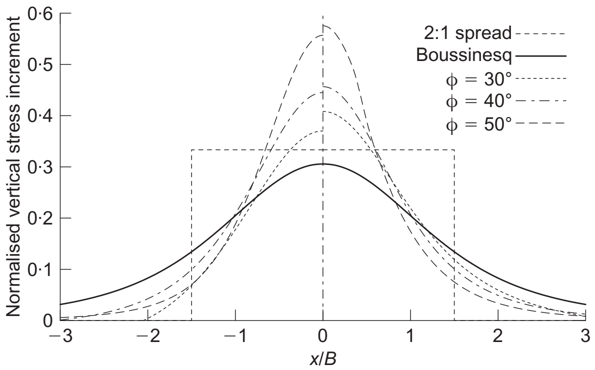

Fig. 10. Normalised vertical stress increment distributions acting at depth $2B$ beneath rough footing. Left-hand side, $q/\gamma B = 0$; right-hand side, $q/\gamma B = \infty$

tions. This has important implications for analyses of loads transmitted through soils to buried structures, where yield conditions are assumed.

NOTATION

- B breadth of footing
- f small change in ψ
- N_q, N'_q, N_γ dimensionless bearing capacity factors
- p ultimate bearing capacity of footing
- q soil surface surcharge stress
- r, θ polar coordinates
- x, y Cartesian coordinates
- γ unit weight of soil
- δ roughness of footing base
- Δ $\sin\delta/\sin\phi$
- ε angle of characteristics to major principal stress direction
- μ superposition correction factor
- σ mean stress
- σ_x, σ_y horizontal and vertical stresses
- τ shear stress
- τ_{xy} horizontal and vertical shear stress
- ϕ angle of shearing resistance
- φ orientation of major principal stress direction to horizontal
- χ $\sigma/\gamma r$
- ψ orientation of major principal stress direction to θ

REFERENCES

Bolton, M. & Lau, C. (1993). Vertical bearing capacity factors for circular and strip footings on Mohr–Coulomb soil. *Can. Geot. J.* **30**, 1024–1033.

Eurocode 7 (1995). *Eurocode 7: Geotechnical design-Part 1: General rules (together with the United Kingdom National Application Document), DD ENV 1997–1:1995*. London: British Standards Institution.

Hansen, B. & Christensen, N. (1969). Discussion of 'Theoretical bearing capacity of very shallow footings', by A. L. Larkins. *ASCE J. Soil Mech. Found. Div.* **95**, No. 6, 1568–1572.

Heurtaux, J. (1959). Sur certains types des singularités des états limites plans des sols pulvérulents. *Comptes Rendus de l'Academie d'Agriculture de France* **249**, No. 23, 2489–2491.

Hjiaj, M., Lyamin, A. & Sloan, S. (2005). Numerical limit analysis solutions for the bearing capacity factor N_γ. *Int. J. Solids Struct.* **42**, 1681–1704.

Ko, H. & Davison, L. (1973). Bearing capacity of footings in plane strain. *J. Soil Mech. Found. Div. ASCE* **99**, No. SM1, 1–23.

Lundgren, H. & Mortenson, K. (1953). Determination by the method of theory of plasticity of the bearing capacity of continuous footings on sand. *Proc. 3rd Int. Conf. Soil Mech. Found. Engng, Zurich* **1**, 409–412.

Martin, C. (2003a). Discussion of 'Calculations of bearing capacity factor N_γ using numerical limit analysis', by Ukritchon, B., Whittle, A. J. and Klangvijit, C., *ASCE J. Geotech. Geoenviron. Engng* **129**, No. 6, 468–474.

Martin, C. (2003b). New software for rigorous bearing capacity calculations. *Proceedings of the British Geotechnical Association international conference on foundations*, Dundee, pp. 581–592.

Sokolovski, V. (1965). *Statics of granular media*. Oxford: Pergamon Press.

Zhu, D., Lee, C. & Law, K. (2003). Determination of bearing capacity of shallow foundations without using superposition approximation. *Can. Geotech. J.* **40**, 450–459.